2012 IACSIT Coimbatore Conferences
IPCSIT vol. 28 (2012) © (2012) IACSIT Press, Singapore

Broadband Second-Harmonic Generation in the Mid-Infrared Region in a Tapered Zinc Telluride Slab Using Total Internal Reflection Random Quasi-Phase Matching

Sumita Deb [1,+], and Ardhendu Saha [2]

[1,2] National Institute of Technology, Agartala, Barjala, Jirania, Tripura (west), Pin-799055, Tripura, India.

Abstract. We analytically describe the concept of broadband second-harmonic generation in the mid-IR region in an isotropic tapered semiconductor slab made of Zinc Telluride (ZnTe) using total internal reflection quasi phase matching. The simulated results indicate an extremely broad spectral bandwidth of 882 nm centered at 7.521μm (7.108 to 7.99 μm) in a 10-mm-long slab with a conversion efficiency of 1.15% while considering the losses due to absorption and surface roughness of the slab. The effects of variations in length, and tapering angle of the semiconductor slab have been studied for the generated second-harmonic radiation.

Keywords: second-harmonic generation, broadband, isotropic, zinc telluride.

1. Introduction

The broadband frequency conversion of laser radiation has manifold applications, from spectroscopy to optical communication, as a broadband source in the desired frequency band. The most important considerations for broadband frequency conversion in any material system are high efficiency and broad bandwidth (BW), which directly depend upon satisfying the phase-matching condition [1]. In this context, quasi-phase matching (QPM) has proven to be the most promising technique because of its ability to phase-match any two waves by choosing an appropriate spatial period of modulation of the nonlinear coefficient along the propagation direction within the transparency region of the chosen material.

With the advancement in the field of semiconductor technology, isotropic semiconductors have arisen as excellent candidates for optical frequency conversion. Among these semiconductors, ZnTe has indeed come forward as an important nonlinear optical crystal, finding wide applications in generation of pulsed terahertz radiation in time-domain terahertz spectroscopy, terahertz imaging, holographic interferometry, optical rectification, reconfigurable optical interconnections, and in laser optical phase conjugation devices [2, 3] However, ZnTe being isotropic, no natural birefringence phase matching is possible. Therefore, QPM may be considered an attractive technique for frequency generation in ZnTe crystal.

It was 1962 when Armstrong *et al.* first suggested that QPM can be obtained by total internal reflection (TIR) in a plane parallel slab [4]. This technique has been demonstrated in isotropic semiconductor (GaAs, ZnSe, ZnS) slabs for resonant-QPMas well as nonresonant QPM by a number of researchers [5-7]. Recently, Baudrier-Raybaut *et al.* have shown that efficient frequency conversion can be achieved in disordered polycrystalline isotropic materials by a random QPM technique [8]. The frequency-converted waves generated by the individual domains of the polycrystalline structure achieve random phases and interfere neither constructively nor destructively, and the output intensity is given as the sum of the intensities due to individual domains. This technique has been demonstrated in transparent (ZnSe) [8] as well as opaque (GaP) [9] semiconductors and indeed has great potential in the field of nonlinear optics for the generation of new frequencies.

[+] Corresponding author. Tel.: +91 9862029099; fax: + 0381-232 6630.
E-mail address: sumita_nita@rediffmail.com.

2. Proposed Scheme

We have considered a tapered semiconductor slab (Fig. 1) of length, L, with the base surface parallel to the horizontal plane while the upper surface is tapered at an angle θ determined by the heights of the two ends t1 and t2, t1< t2. The face on which the fundamental laser radiation will be incident is cut at an angle ψ with respect to a plane perpendicular to the horizontal plane.

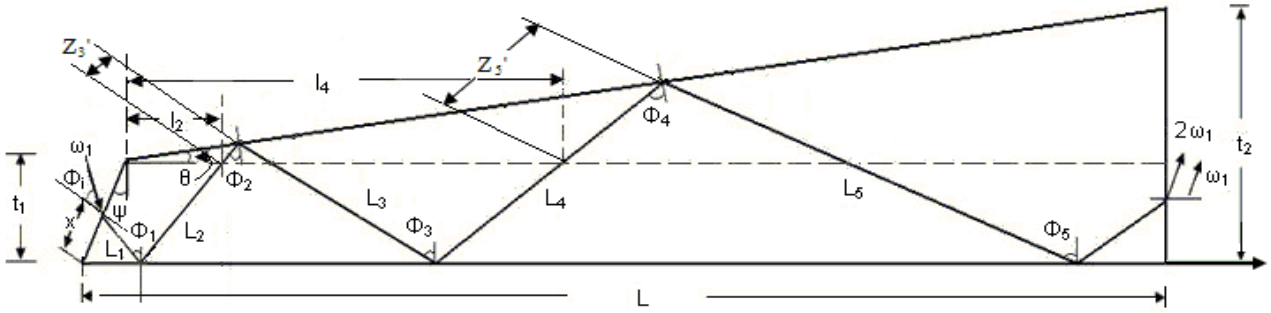

Fig. 1. Geometry of tapered semiconductor slab showing the scheme of second harmonic frequency conversion.

Let the fundamental broadband optical radiation having centre frequency ω1 be incident at an angle φi with respect to the normal to the inclined slab end face. The angle of incidence φ1 on the horizontal plane inside the semiconductor slab will be determined by the refractive index of the material. If φ1 is greater than the critical angle for the range of input frequencies, then the collimated optical radiation will undergo TIR inside the tapered slab. Here the angle of incidence and the length between successive bounces will continue to increase with the propagation of the input broadband radiation throughout the length of the tapered semiconductor slab. This scheme corresponds to non-resonant QPM since the interaction lengths between successive bounces cannot be optimized to be equal to an odd multiple of the coherence length Lcoh (=π/Δk, where Δk is the dispersive wave-vector mismatch) for all the frequencies available in the input band of the fundamental laser radiation. However, a situation may arise wherein one length may coincide with an odd multiple of the coherence length of a particular frequency in the input band of the fundamental waves, whereas another length may coincide with an odd multiple of the coherence length of another frequency in the band, and so forth. The conversion efficiency for that particular frequency will be higher for that particular interaction length since it will then correspond to resonant QPM. However, the conversion efficiencies of other frequencies will be lower for that interaction length owing to non-resonant QPM. The phase shifts of the interacting waves indeed vary randomly during their propagation inside the slab, thereby giving rise to a situation identical to that of random QPM, wherein the constructive as well as the destructive interference effects of the interacting waves are destroyed. Clearly, the proposed scheme is less efficient than the truly phase-matched condition because the latter benefits from the constructive interference of the waves generated by different parts of the nonlinear medium, but it outperforms the phase-matched scenario for which the interference of the generated waves is destructive, thereby resulting in a flatter spectral BW.

2.1. Mathematical Analysis

Now, in this tapered slab configuration with simple geometry the equation for the length between consecutive bounces can be expressed in terms of slab parameters as follows:

$$L1 = x\cos\psi/[\sin(\varphi r+\psi)] \quad (1)$$

where L_1 is the length between the entrance point and the point of first TIR point inside the slab, x is the slant distance of the entrance point from the base of the slab, and $\varphi_r = \sin^{-1}[(\sin\varphi_i)/n_k]$, where n_k is the refractive index corresponding to each individual frequency of the input broadband laser radiation.

The distance between successive bounces can be expressed by the following coupled equations:

$$l_2 = x\sin\psi + (x\cos\psi\ \tan\varphi_1) + t_1\tan\varphi_1 - t_1\tan\psi$$

$$z'_{2n-1} = (l_{2n-2}\sin\theta)/\cos\varphi_{2n-2},\ n = 2, 3...n_{tot}$$

$$l_{2n} = l_{2n-2} + z'_{2n-1}\sin\varphi_{2n-3} + [(z'_{2n-1}\sin\varphi_{2n-3})/\tan(\pi/2 - \varphi_{2n-1})] + 2t_1\tan\varphi_{2n-1},\ n= 2, 3...n_{tot}$$

$$z'_{2n+1} = (l_{2n}\sin\theta)/\cos\varphi_{2n},\ n = 1, 2, 3...n_{tot}$$

$$L_{2n} = (t_1/\cos\varphi_{2n-1}) + [(l_{2n}\sin\theta)/\cos\varphi_{2n}],\ n = 1, 2, 3...n_{tot} \quad (2)$$

$$L_{2n+1} = (t_1/\cos\varphi_{2n+1}) + [(z'_{2n+1}\cos_{2n-1})/\cos\varphi_{2n+1}),\ n = 1, 2, 3...n_{tot} \quad (3)$$

Here,
$$\theta = \tan^{-1}[(t_1-t_2)/L] \quad (4)$$

$$\varphi_n = (n-1)\theta + \varphi_1,\ n = 1, 2, 3...n_{tot}, \quad (5)$$

where $\varphi_1 = \pi/2 - (\varphi_r + \psi)$ and n_{tot} is the total number of bounces inside the tapered slab.

2.2. Polarization Configuration

In our analysis we consider the ppp polarisation configuration. ZnTe belongs to symmetry class $\bar{4}3m$. We have used the approximate value of d_{14}=90 pm/V for ZnTe crystal [l0].

2.3. Conversion Yield Limiting Factors

The SHG conversion efficiency is limited by three important factors: the surface roughness, the Goos-Hänchen shift, and the absorption loss of the material. All these factors are considered in our analysis.

The drop due to residual surface roughness is measured in terms of the Strehl ratio [7, 11], which gives the reflection coefficient, R as a function of wavelength, angle of incidence, and standard deviation,

$$R = \exp[-\{(4\pi n_j\sigma\cos\varphi_n)/\lambda_j\}^2] \approx 1- \{(4\pi n_j\sigma\cos\varphi_n)/\lambda_j\}^2 \quad (6)$$

where j = ω for the fundamental wave and 2ω for the generated SH, and σ(= p—v value/12) [12] where the p—v value is the distance between the peak and valley of the surface under consideration. A p—v value of 30 nm is considered in the computer-aided simulation [13].

When a collimated light beam is totally reflected from a plane interface between two dielectric media, the reflected beam encounters a longitudinal shift between the incident and reflected beams known as the Goos-Hänchen (GH) shift) [14]. This longitudinal shift causes a reduction of the usable length of the semiconductor slab. In our case, the GH shift has been separately calculated for the lower horizontal surface and the inclined upper surface.

Linear absorption can be highly detrimental to frequency conversion processes and places severe limits on conversion efficiency values. In our analysis we consider a linear absorption coefficient ($\alpha_\omega \approx \alpha_{2\omega}$) 0.008$cm^{-1}$ for ZnTe crystal [10].

2.4. SH Intensity

The SHG intensity $I_{2\omega}$ for the undepleted pump and plane wave approximation is calculated individually for each interaction length using the relation

$$I_{2\omega}=\{(8\pi^2 d_{eff}L^2I_\omega^2)/(\varepsilon_o c n_{2\omega}n_\omega^2\lambda_\omega^2)\}\exp[\{\alpha_\omega+(\alpha_{2\omega}/2)\}L][\sin^2(\Delta kL/2)+\sinh^2\{\alpha_\omega-(\alpha_{2\omega}/2)\}L/2]/[(\Delta kL/2)^2+\{\alpha_\omega-(\alpha_{2\omega}/2)\}L/2\}^2], \quad (7)$$

All these values of $I_{2\omega}$ are summed to obtain the final output intensity for a particular wavelength. In our analysis the interaction length between the last bounce and the exit point from the semiconductor slab is not considered. The effects of linear absorption and surface roughness on both the fundamental and the generated SH waves are included for all the consecutive bounces inside the slab. The reduction in the usable length of the semiconductor slab due to the GH shift is also considered in the analysis. The dispersion equation of ZnTe [15], has been used to calculate the refractive indices corresponding to fundamental and SH for the range of frequencies available in the input broadband source.

3. Results and Discussions

In the computer-aided simulation, the input beam intensity is assumed to be $I_\omega \approx 10$ MW/cm^2. The analysis uses an input fundamental broadband source of 6.8−8.2 μm. The slab dimensions are set asL = 10 mm, t_1 = 1000 μm, and t_2 = 1010 μm. The input conditions at the entry point of the collimated optical beam to the semiconductor slab are chosen as ϕ_i = 1.1 rad and x = 100 μm. The variation of SH efficiency with respect to the input fundamental wavelength is shown in Fig. 2. The analytical results thus obtained indicate the possibility of an extremely wide spectral BW of 887 nm in the tapered slab under ideal conditions, neglecting all the losses. However, when the effects of the surface scattering, absorption, and GH shift of the

interacting waves are taken into account, the BW is reduced to 882 nm. The SH conversion efficiency drops by 16% relative to its value under no-loss condition.

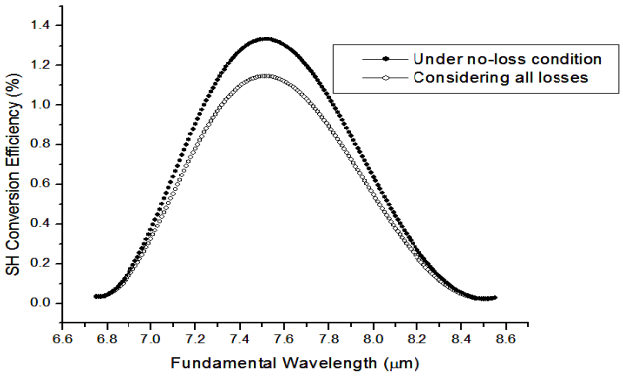

Fig. 2. Plot of SH efficiency vs input wavelength for the tapered ZnTe slab for ψ = 0.6 rad, ϕi= 1.1 rad, L =10 mm, t1= 1000 μm, and t2 =1010 μm: (a) under no-loss condition and (b) considering all the losses (scattering, absorption, GH shift) encountered by the interacting waves.

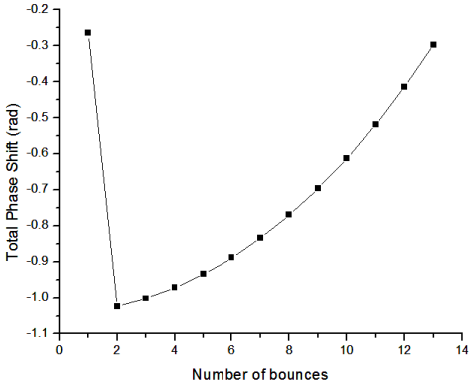

Fig. 3.Variation of net phase shift encountered by the interacting waves at each TIR bounce inside the tapered slab corresponding to the centre wavelength (7.521μm) of the fundamental beam.

For the tapered slab, since the lengths between the consecutive bounces and also the angle of incidence at each bounce change with the progression of the collimated beam inside the slab, the net phase shift at each bounce is given as $\Delta\phi = \Delta k L_i + \Delta\phi_F$, where L_i is the interaction length between two consecutive bounces, and $\Delta\phi_F = \phi_p^{2\omega} - \phi_p^{\omega}$, where $\phi_p^{2\omega}$ and ϕ_p^{ω} denote the Fresnel phase shifts encountered at TIR by the SH and fundamental waves respectively. This value of $\Delta\phi$ is rapidly varying (Fig. 3), thereby destroying the interference effect among the generated waves. This eventually results in a flatter spectral response at the cost of lower conversion efficiency.

We studied the effects of varying the tapering angle and slab length on the generated SH efficiency and the fundamental bandwidth for the tapered ZnTe slab under consideration.

3.1. Variation of tapering angle

The tapering angle θ of the slab can be varied by changing the second height t_2 (Fig.1) of the slab while keeping the first height t_1 constant at 1000 μm. With increasing $(t_2 - t_1)$, θ increases, resulting in the broadening of the 3 dB BW, with a drop in conversion efficiency. When $(t_2 - t_1)$ is increased from 10 to 30 μm, the BW broadening is 67 nm, while the relative drop in the peak conversion efficiency is about 23%. The analytical results are shown in Table I.

Table I. Variation in performance parameters with increase in height t2 for L = 10 mm, ϕi= 1.1 rad, and t1=1000 μm.

t_2-t_1(μm)	SH conversion efficiency (%)	3 dB BW (nm)
10	1.15	882
20	1.05	894
30	0.996	949

3.2. Variation of slab length

With increasing crystal length, the SH conversion efficiency improves but its BW shows slight decrease. Table II shows the analytical results for the variation in length of the slab. As the length is increased from 10 to 20 mm, the SH conversion efficiency increases relatively by 70% while the BW drops by only 12 nm.

Table II. Effect of variation in performance parameters with slab length L for Φi= 1.1 rad, t1=1000 μm, and t2=1010μm.

Slab length L (mm)	SH conversion efficiency (%)	3 dB BW (nm)
10	1.15	882
15	1.612	874
20	1.96	870

4. Conclusion

To conclude in this paper, a broadband frequency converter based on a tapered ZnTe slab has been analysed numerically. The converter provides an extremely wide 3 dB BW of 882 nm (approximately 7.108 to 7.99 μm), centred at 7.521 μm, in the mid-IR region, with a SH conversion efficiency of 1.15 %, while considering the losses. The proposed frequency converter may be considered as a simple yet competitive means of obtaining extremely wide broadband SHG based on ZnTe isotropic crystal.

5. References

[1] M. M. Fejer, G. A. Magel, D. H. Jundt, and R. L. Byer, Quasi-Phase-Matched Second Harmonic Generation: Tuning and Tolerances. *IEEE J. Quantum Electron*. 1992, **28**: 2631-2654.

[2] S. M. Harrel, R. L. Milot, J. M. Schleicher, and C. A. Schmuttenmaerc, Influence of free-carrier absorption on terahertz generation from ZnTe (110). *J. Appl. Phys.* 2010, **107**: 033526-1- 033526-5.

[3] http://en.wikipedia.org/wiki/ZnTe

[4] J. A. Armstrong, N. Bloembergen, J. Ducuing, and P. S. Pershan, Interactions between light waves in a nonlinear dielectric. *Phys. Rev*. 1962, **127**: 1918-1939.

[5] G. D. Boyd and C. K. N. Patel, Enhancement of optical second harmonic generation (SHG) by reflection phase-matching in ZnS and GaAs. *Appl. Phys. Lett.* 1966, **8**: 313-315.

[6] H. Komine, W. H. Long, Jr., J. W. Tully, and E. A. Stappaerts, Quasi-phase-matched second-harmonic generation by use of a total-internal-reflection phase shift in gallium arsenide and zinc selenide plates. *Opt. Lett.* 1998, **23**: 661-663.

[7] R. Haïdar, N. Forget, P. Kupecek, and E. Rosencher, Fresnel phase matching for three-wave mixing in isotropic semiconductors. *J. Opt. Soc. Am. B.* 2004, **21**: 1522-1534.

[8] M. Baudrier-Raybaut, R. Haïdar, Ph. Kupecek, Ph. Lemasson, and E. Rosencher, Random quasi-phase-matching in bulk polycrystalline isotropic nonlinear materials. *Nature.* 2004, **432**: 374-376.

[9] V.A. Mel'nikov, L.A. Golovan, S.O. Konorov, D.A. Muzychenko, A.B. Fedotov, A.M. Zheltikov, V.Yu. Timoshenko, and P.K. Kashkarov: Second-harmonic generation in strongly scattering porous gallium phosphide *Appl. Phys. B.* 2004, **79**: 225-228.

[10] http://www.clevelandcrystals.com/II-VI.htm

[11] P. K. Tien, Light waves in thin films and integrated optics *Appl. Opt.* 1971, **10**: 2395-2413.

[12] R. Haïdar, P. Kupecek, E. Rosencher, R. Triboulet, and P. Lemasson, New mid-infrared optical sources based on isotropic semiconductors (zinc selenide and gallium arsenide) using total internal reflection quasi-phase-matching. *Opto-Electron. Rev*. 2003, **11**: 155-160.

[13] N. Lovergine, D. Manno, A. M. Mancini, and L. Vasanelli, Surface structural and morphological characterization of ZnTe epilayers grown on {100} GaAs by MOVPE. *J. Cryst. Growth*. 1993, **128**: 633-638.

[14] A. W. Snyder and J. D. Love, Goos-Hänchen shift. *Appl. Opt*. 1976, **15**: 236-238.

[15] D. T. F. Marple, Refractive index of ZnSe, ZnTe, and CdTe. *J. Appl. Phys*. 1964, **35**: 539-542.